

## **Detection of shaft-seal rubbing in large-scale power generation turbines with Acoustic Emissions; Case study**

**D. Mba<sup>1</sup>, A. Cooke<sup>2</sup>, D. Roby<sup>3</sup>, G. Hewitt<sup>3</sup>**

<sup>1</sup>School of Engineering, Cranfield University, Cranfield, Beds, MK43 0AL, UK

<sup>2</sup>Humber Power Ltd, Stallingborough, North East Lincolnshire, DN41 8BZ. UK

<sup>3</sup>Power Technology, Powergen, Nottingham, NG11 OEE. UK

### **Abstract**

Rubbing between the central rotor and the surrounding stationary components of machinery such as large-scale turbine units can escalate into severe vibration, resulting in costly damage. Although conventional vibration analysis remains an important condition monitoring technique for diagnosing such rubbing phenomena, the non-destructive measurement of Acoustic Emission (AE) activity at the bearings on such plant is evolving into a viable complementary detection approach, especially adept at indicating the early stages of shaft-seal rubbing. This paper presents a case study on the application of high frequency acoustic emissions as a means of detecting and verifying shaft-seal rubbing on a 217MVA operational steam turbine unit. The generation of AE activity is attributed to the contact, deformation, adhesion and ploughing of surface asperities on the rubbing surfaces of the rotor and stator.

**Keywords-** Acoustic emissions, condition monitoring, power generation turbines, rub diagnosis, shaft-seal rubbing

## **1. Introduction**

Rubbing is an undesired contact between a rotating and stationary part and usually occurs as a secondary effect of some machine malfunctions such as unbalance, misalignment, thermal expansion and fluid-induced self excited vibration. Rotor-Stator rubbing may be broadly classified as either partial or continuous. The former type describes brief intermittent contacts and the latter describes more sustained contact between rotor and stator. Partial rubbing can often occur at a constant shaft location due to the combined effects of modal vibration and the orbital motion of the rotor. Such periodic rub events at a constant location on the shaft can induce a differential temperature gradient, leading to a local thermal expansion that causes the shaft to bow. Rubbing in large steam turbines is not an uncommon occurrence. Vibration characteristics symptomatic of light radial rubbing are observed mainly during transient operation (e.g. load-ups). This type of rubbing can be tolerated provided the vibration levels remain well within acceptable criteria. However, there are occasions when the rubbing becomes severe enough for the machine to be removed from service to rectify the cause of the rubbing.

The most common method of diagnosing shaft-seal rubbing is vibration monitoring of the bearing pedestals via accelerometers and velocity transducers. Generally a certain level of rotor dynamics knowledge is required for accurate diagnosis of rubbing. However, the use of vibration monitoring only identifies that rubbing is taking place; what the Engineer actually requires is the location of the rubbing so that remedial repairs can be undertaken. Quite often it is not obvious from the changing pattern of vibration to identify the offending cylinder, particularly if rubbing occurs at one end

of a cylinder, and due to the dynamic characteristics, has a strong influence on the vibration of adjacent cylinders. In a review of monitoring techniques applied to steam turbine units [2,3], acoustic emission (AE) was identified as a condition monitoring technique that might potentially detect the sliding contact between rotating and stationary components.

## **2. Acoustic Emission**

Acoustic Emission is defined as the resulting transient elastic wave generated when strain energy is released suddenly within or on the surface of a material. This is due to microstructure changes, i.e., dislocations, crack generation and propagation, friction phenomena, fibre breakage, etc. These changes can be generated internally or externally and cover a broad frequency range between 20 KHz to several Mega-Hertz. The application of the acoustic emission technique in research and industry is well-documented [4,5]. It has traditionally been used for monitoring defects in statically loaded structures [6,7,8], but it has found increasing application in non-destructive monitoring of bearings [9,10,11,12,13,14] and in indicating the loss of mechanical integrity in very slow rotating plant [15,16,17].

In this paper only AE generated from the process of friction and wear on the rubbing faces of the rotor and stator is considered. Typically AE covers a frequency range of 100KHz to 1Mega-Hertz. The relationship between AE and wear arose from attempts to establish movements of a work piece in respect to the tooling, for instance, during the machining process. The generation of AE during the sliding motion of two mating

surfaces is attributed to adhesion, contact and deformation of asperities and the ploughing action of wear particles [18]. It has been shown [18,19,20,21,22] that the strength and rate of AE activity is dependent on sliding velocity, friction coefficient of mating surfaces, contact pressure and the height of surface roughness. In addition, these studies have been undertaken with and without lubrication. It may be concluded that the process of rubbing between stator and rotor will generate AE activity.

On operational machines it is often only practical to take AE measurements from non-rotating members, such as the bearing housing. Consequently, AE signals originating from the rotating shaft will incur significant attenuation across the transmission path to the receiving AE transducer. This attenuation can be attributed to geometrical spreading across the surface or volume of the rotor, and, acoustic reflections at the bearing interfaces caused by acoustic impedance mismatches. Moreover, the AE signal will be further coloured by the characteristic frequency response of the AE transducer. However, Mba et al [23] have confirmed the transmissibility of AE waves across turbine rotors. To date a limited amount of research has been undertaken on the application of AE to monitoring shaft seal rubbing on operational power generation turbine units.

### **3. Application of Acoustic Emission to seal rubbing**

Sato [24] investigated the use of AE to monitor seal rubbing on an operational 350MW steam turbine. AE sensors were attached to adjacent journal bearings whilst continuous rubbing was introduced at various rotor locations between the bearings with an aluminium sample. During tests on the steam turbines it proved difficult to judge rubbing phenomena solely on amplitude changes due to high background noise. However, Sato used the spectrum of the envelope AE waveform and showed that rotational frequencies of the turbine were generated with rubbing. The above-mentioned procedure was also successful in detecting bearing tilt under considerable background noise. Furthermore, Sato found that the rub source location could be determined using the time or phase difference between the AE modulated signals from two sensor channels on adjacent bearings.

Board [25] applied stress wave analysis for diagnosis of seal rubbing on a turbine unit. The generation of stress waves was attributed to the friction, shock and dynamic load transfer between moving parts in rotating machinery. The frequency range of stress waves employed was centred at 40kHz. In the particular case presented, it was stated that observations were made on an operational steam turbine unit over a 5-month period during which a stress wave sensor, placed on a Low Pressure Turbine bearing, showed what was described by Board as ‘erratic’ activity. This was attributed to an increase in friction levels although no measured or characteristic indicators from stress wave signatures were given. It was stated that on disassembly there was evidence of excessive wear to the face of the labyrinth seals.

Wang's [26] investigation on rub location was centred on a test-rig and two AE sensor were employed to aid source identification. It was surprising that whilst the AE sensor employed had a frequency range of between 20 kHz to 1.5MHz, a sampling rate of less than 20 kHz was employed. However, Wang noted that the envelope of the AE signature indicated rubbing phenomenon, as observed by Sato [24]. Furthermore, it was stated that due to the influences of impacting, structural characteristic, oil film and noise, a conventional cross-correlation technique was unable to aid identification of the rub source, however, success was claimed using a wavelet transform cross-correlation method.

Miettinen et al [27] applied AE to monitoring sliding contact behaviour of mechanical face seals on a 15KW centrifugal pump. It was concluded that AE amplitude values of a leaking seal were on average 25% lower than in normal running conditions. The authors stated the results were not surprising considering that in operation the seal face contact could experience boundary or mixed film lubrication regimes. Tests on dry running conditions for the seal faces indicated an even higher level of AE amplitude.

The application of AE to diagnosis of seal rubbing on operational turbine unit's [24] and on a test-rig [26] has shown a direct correlation between AE envelope signature and rubbing.

#### 4. Acquisition experiment and measurement procedure

A schematic diagram of the acquisition system is illustrated in figure 1. A commercially available broadband piezoelectric transducer with a measurement bandwidth of 100 kHz -1 MHz was employed. The acquisition board was the Physical Acoustics Corporation AE-DSP-32/16 card set with a sampling rate of 4MHz and 16-bit precision. The receiving transducer was connected to a pre-amplifier (set at 60dB gain), which was in turn connected to the acquisition board. In addition, the acquisition system employed an 8<sup>th</sup> order Butterworth anti-aliasing filter with a 3dB roll-off at 1.2MHz.

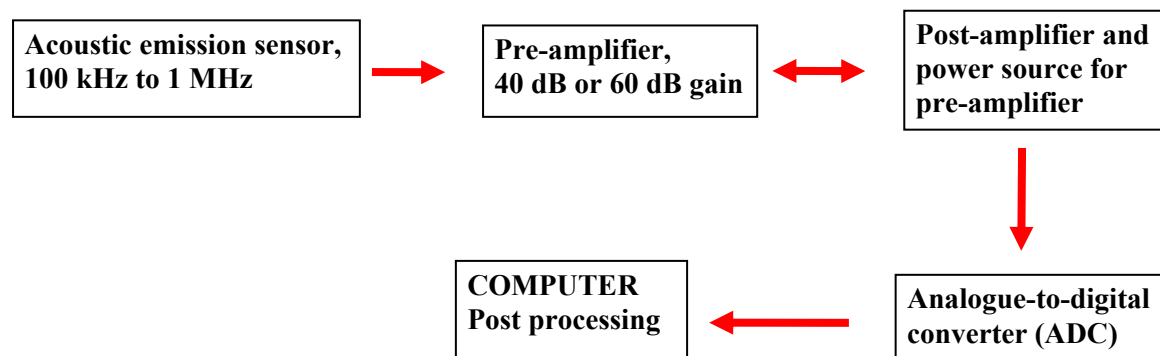


**Figure 1** Schematic diagram of acquisition system

The system provided a total of 32,000 data points for recording. Two sets of AE signatures were taken for each of the gland casings (described further in section 5); the first sampled at 4MHz and the second at 1MHz. All time signatures displayed with corresponding frequency spectra were digitised at 4MHz, whilst time signatures displaying AE data over 0.032sec (1.5 revolutions) were sampled at 1MHz. For all recordings undertaken at the four seal/gland positions the sensor was placed on top of the gland/seal casing, see figure 2, as there was a direct path from the seals to the

casing via spring rings placed between the casing and the seal. This ensured that the transmission paths at all seal casings were identical; however, the location of the sensor on top of each casing was not identical. Whilst theoretically there may be some attenuation due to geometric spreading, this is considered insignificant, particularly as the difference in sensor locations on all the casings could not have been more than approximately 15cm. The spring rings are used to maintain a tight clearance between the seal and the rotor. A magnetic clamp was employed to secure the AE receiving transducer onto the casing. For all recordings a trigger level of 1.75V was set to reduce the amount of noisy AE data.

## **5. Case study**

A brief summary of the investigation into the applicability of AE as a detection tool for shaft seal rubbing on a specific steam turbine is presented. During operation high levels of shaft displacement were noted across the low-pressure turbine cylinders (designated 'LP' in figure 2) and the generator. A rub was suspected as the cause for such high displacement levels. These displacements were observed with permanently positioned eddy current probes. The operational performance of the unit during this condition included a steam exhaust temperature of 18<sup>0</sup>C and a maximum load of 80MW. The rotational speed of the unit was 3000 rpm (50Hz). Acoustic Emission recordings were undertaken at 'LP2 Rear', 'LP2 Front', 'LP1 Front' and 'LP1 Rear', see figure 2.

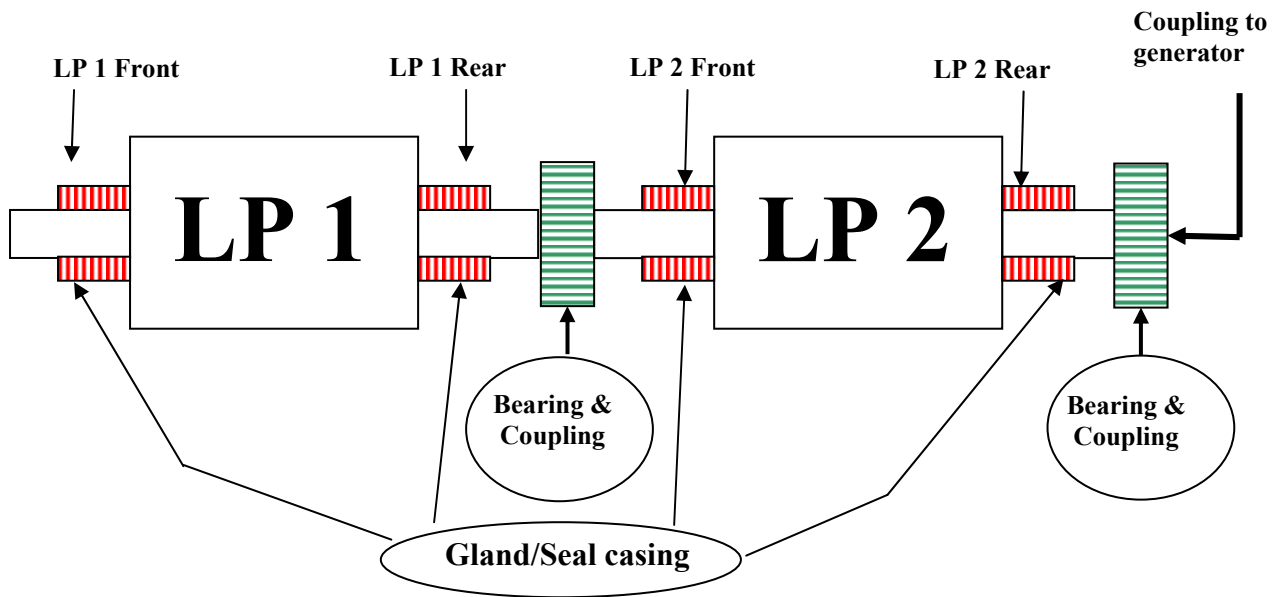


**Figure 2 Schematic of part of the Steam turbine unit**

## 6. Results

A total of 76 AE data files, sampled at 1MHz, were recorded at each of the seal casings. In the following sections AE amplitude modulation has been related to the periodicity of the turbine unit. Results on the modulation frequency in relation to the periodicity of the unit were reached following observations on all recorded AE data. . It must be noted that at 3000rpm (50Hz), one period of shaft rotation corresponded to 0.02seconds.

## 6.1 'LP 2 Rear'

The larger amplitude AE burst signatures detected at this position were generated at 0.02 second intervals, equivalent to the rotational speed of the unit, 50Hz, see figure 3. In addition, smaller amplitude AE burst signatures were emitted between the larger amplitude bursts described above, at a periodicity also equivalent to once-per-revolution, see figure 3. It was noted that the periodicity of all AE transient events was twice the rotational speed. Figure 4 is a close-up view of a selected portion of figure 3 (middle diagram), primarily to show the reader that the transient bursts are not electronic spikes.

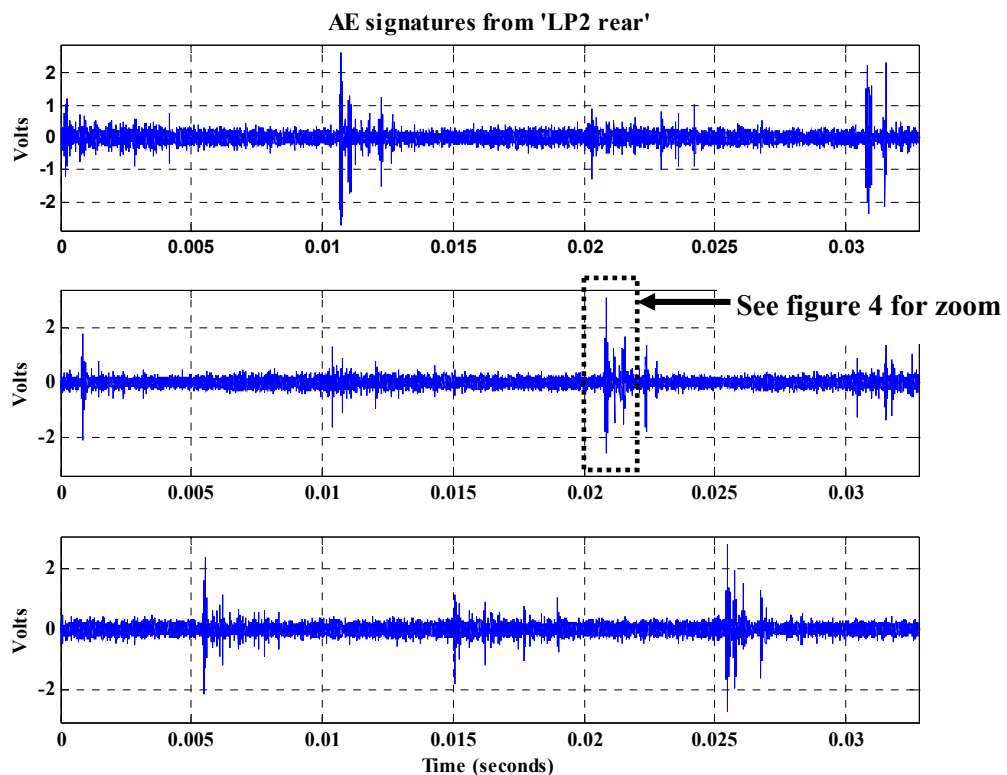


**Figure 3** Typical AE signature from 'LP 2 Rear' (sampled at 1MHz)

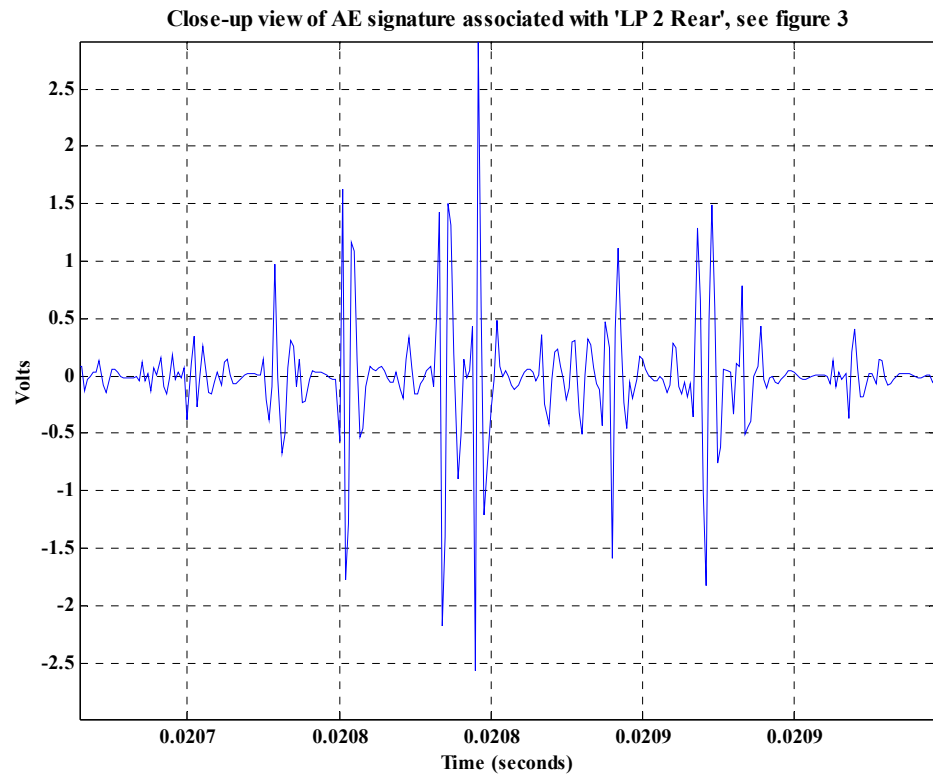


**Figure 4      Close-up view of a selected region in figure 3**

A time signature, with corresponding frequency spectrum, of a typical AE burst signature associated with 'LP2 Rear' can be seen in figure 5. The frequency spectrum ranged from 100kHz to 600kHz.

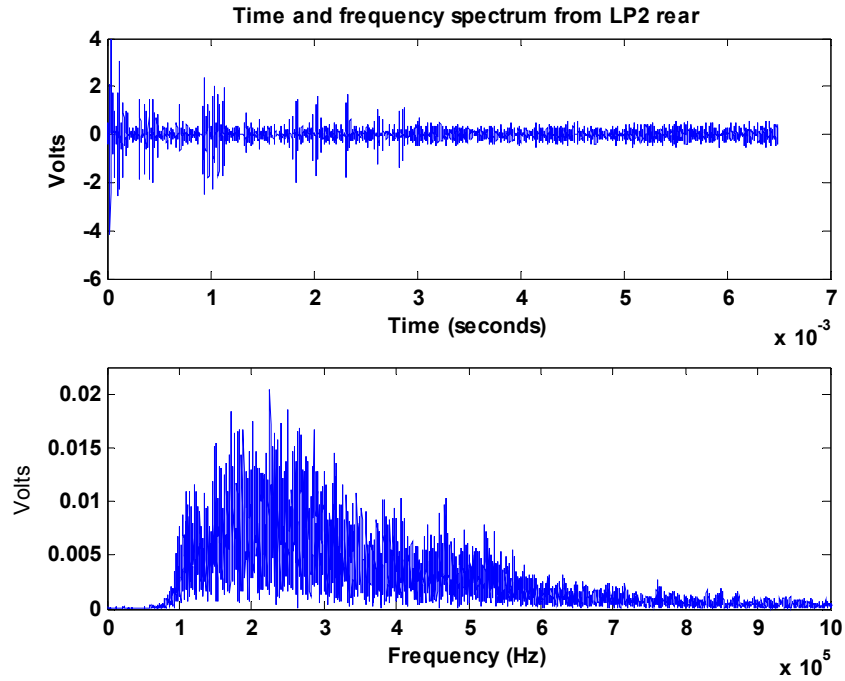


**Figure 5** AE signature from ‘LP 2 Rear’ with corresponding frequency spectrum (sampled at 4MHz)

## 6.2 ‘LP 2 Front’

The AE signatures detected at this position were of larger amplitude and energy than at ‘LP2 Rear’. The high frequency AE burst signatures detected were modulated at twice rotational speed of the rotor, 0.01 seconds or 100Hz, see figure 6. An AE time signature with corresponding frequency spectrum of a typical AE burst at ‘LP2 Front’ can be seen in figure 7. The frequency spectrum of these AE signatures ranged from 100kHz to 600kHz.

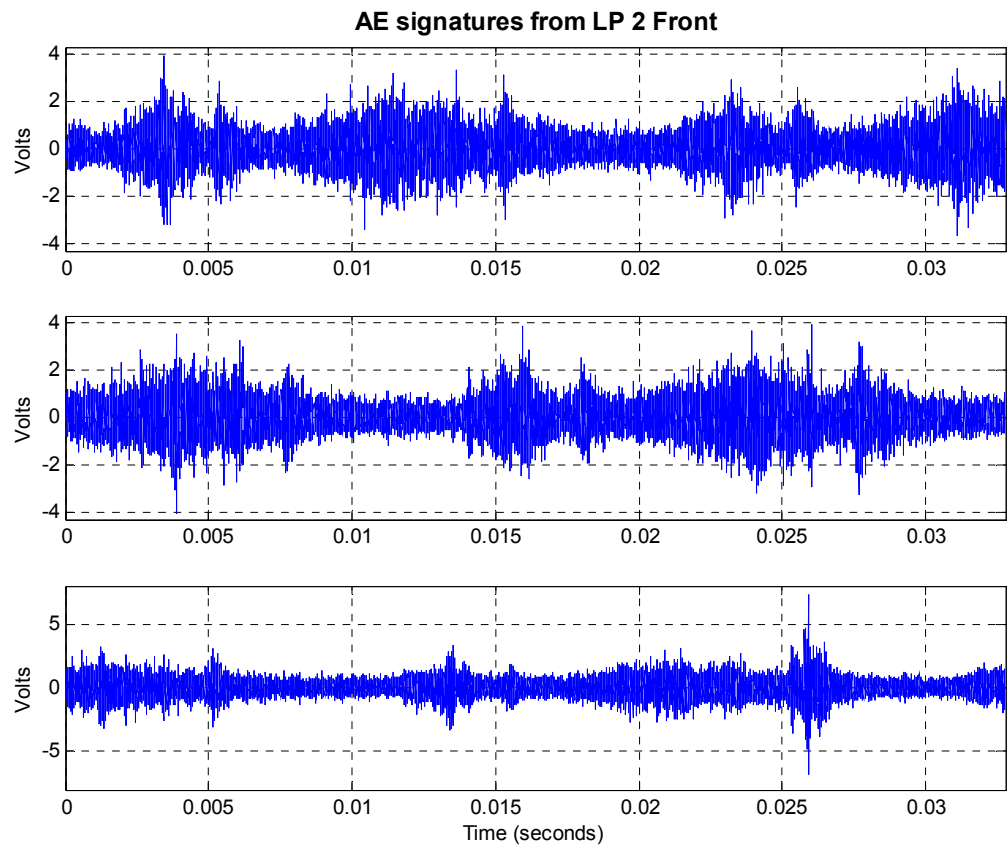


**Figure 6** Typical AE signature from ‘LP 2 front’, (sampled at 1MHz)

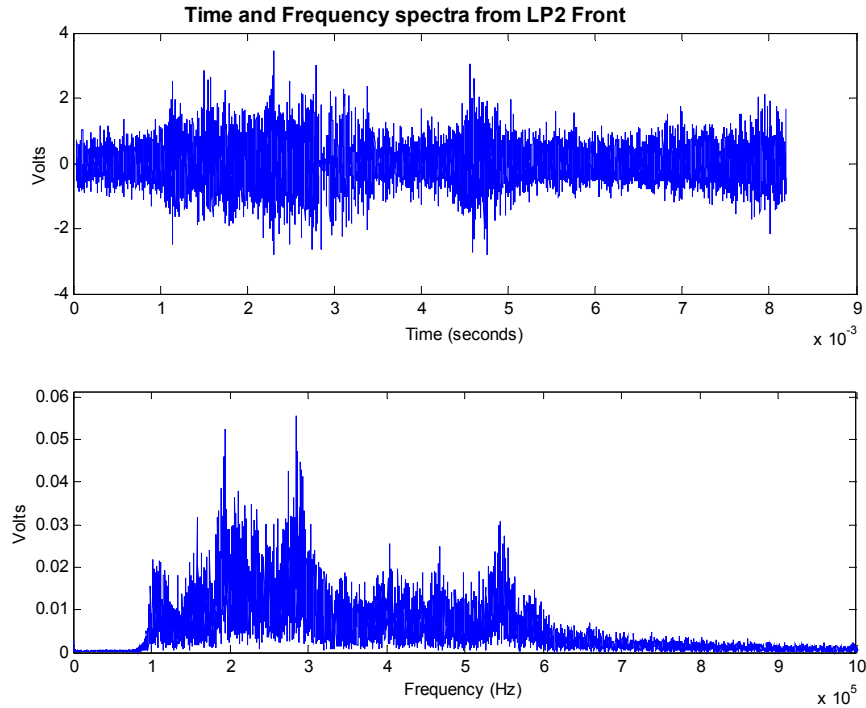


**Figure 7** AE signature from ‘LP 2 Front’ with corresponding frequency spectrum (sampled at 4MHz)

### **6.3 ‘LP 1 Rear’**

High frequency AE burst signatures were detected at 0.02 second intervals, equivalent to the rotational speed of the rotor, 50 Hz, see figure 8. In addition, AE signatures of relatively lower amplitude and energy were evident between the larger amplitude bursts. This phenomenon was observed at ‘LP2 Rear’, although at much lower AE energy levels.

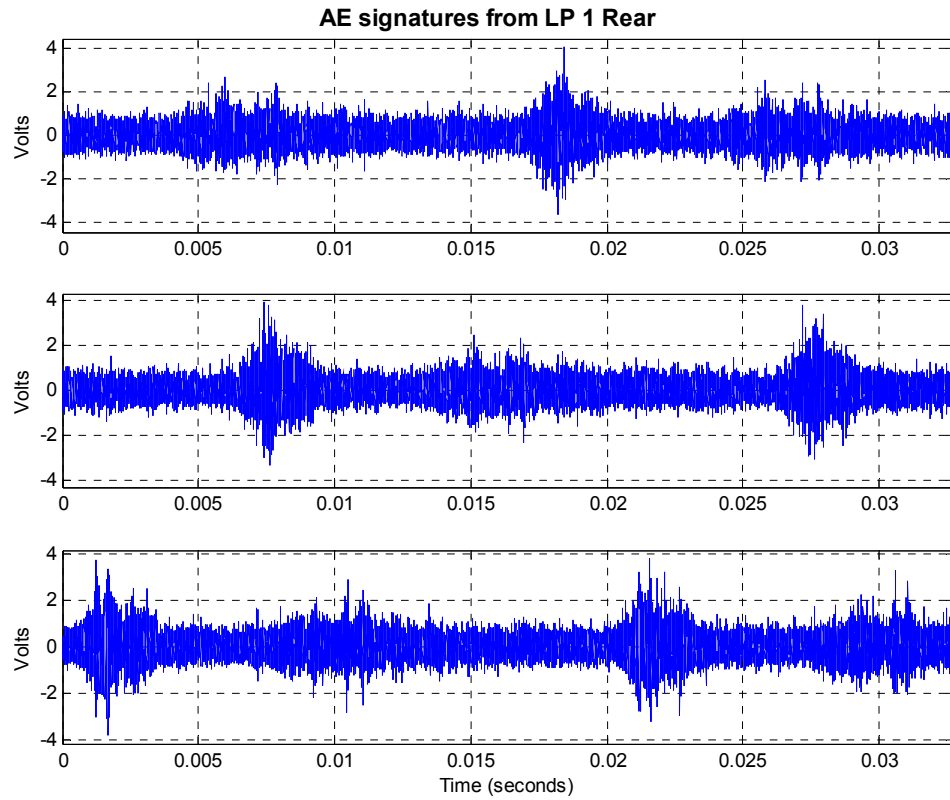


**Figure 8** AE signature from 'LP 1 Rear', (sampled at 1MHz)

A time signature, with corresponding frequency spectrum, of a typical AE burst signature associated with 'LP1 Rear' can be seen in figure 9. The frequency spectrum ranged from 100kHz to 600kHz.

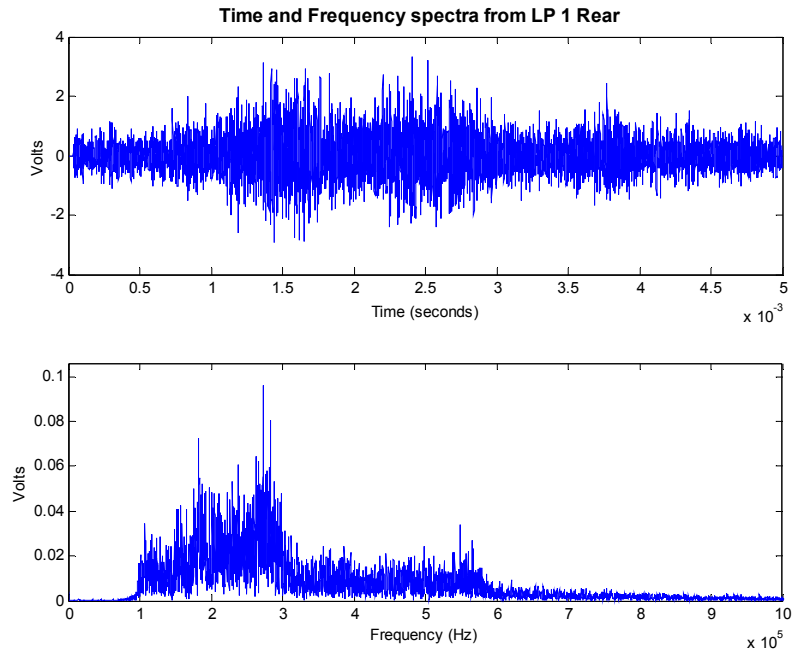


**Figure 9 Typical AE signature from ‘LP 1 Rear’ with corresponding frequency spectrum (sampled at 4MHz)**

#### **6.4 ‘LP 1 Front’**

No AE signatures were detected above the trigger level set at 1.75Volts.

#### **6.5 Other observations**

The operating conditions of the cylinders were modified to reduce the dynamic shaft displacement to acceptable operational levels. This was achieved by reducing the system vacuum thereby causing a rise in steam exhaust temperature and thus an increase in clearance between the seals and the rotor. The performance parameters at this condition included an exhaust temperature of 25°C at a load of 80MW. During the second visit the unit was operating under the conditions detailed above.

Acoustic Emission signatures captured on the second visit from positions ‘LP1 Rear’ and ‘LP2 Front’ showed neither modulation nor distinct discrete AE signatures as was observed during the period of high vibration, see figures 10 and 11. In addition, the amplitude and energy levels of the AE’s observed at the second visit were higher than those recorded in the first visit. This is attributed to the change in operating background noise characteristics and suggests that AE activity is related to the operating conditions of the turbine unit within its cylinder.

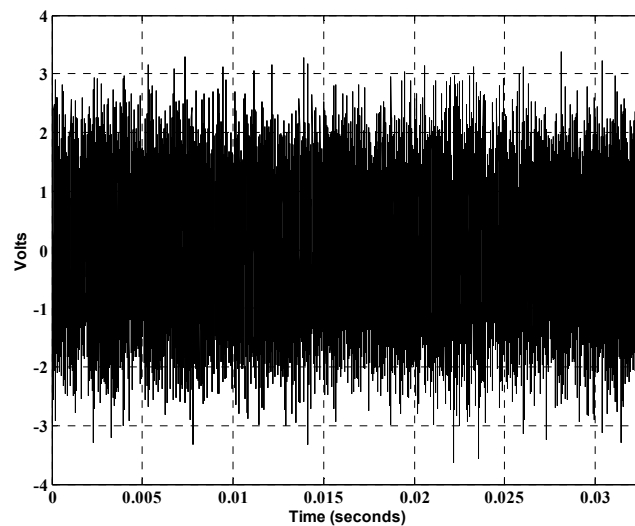


**Figure 10** Typical AE signature detected at ‘LP1 Rear’ after shaft displacement levels had been reduced due to changes in operating conditions.

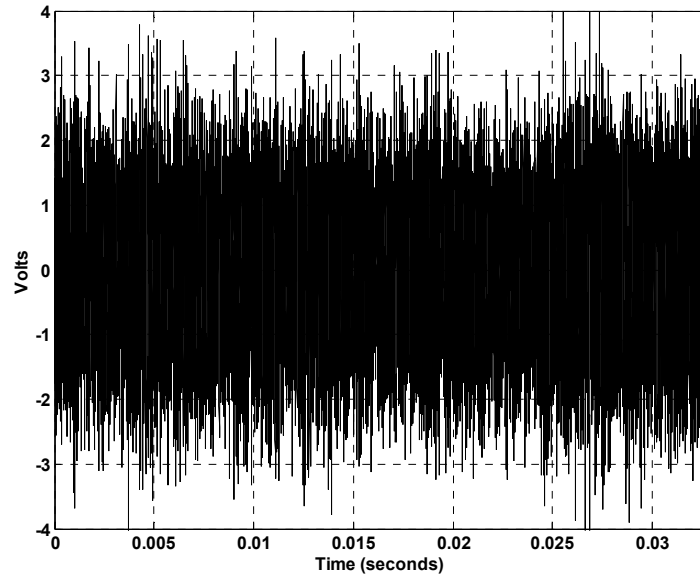


**Figure 11 Typical AE signature detected at ‘LP2 Front’ after shaft displacement levels had been reduced due to changes in operating conditions.**

## **6.6 Source identification**

To aid identification of the main source of rub from the first visit, comparisons of maximum amplitude and energy levels were made on AE signatures from the various seal/gland casings, see figures 12 and 13. A complete breakdown of maximum amplitude and energy values is detailed in appendix A. A total of seventy-six (76) AE data files, each of 0.032 seconds duration, are presented. This was considered sufficient in providing an indication of AE maximum amplitude and energy levels for the three seal casings. Maximum amplitude and energy values were obtained from the entire duration of each data file. The energy was calculated using the trapezoidal numerical integration.

Comparison of AE energy levels from 'LP 2 Front and Rear'  
and 'LP 1 Rear'

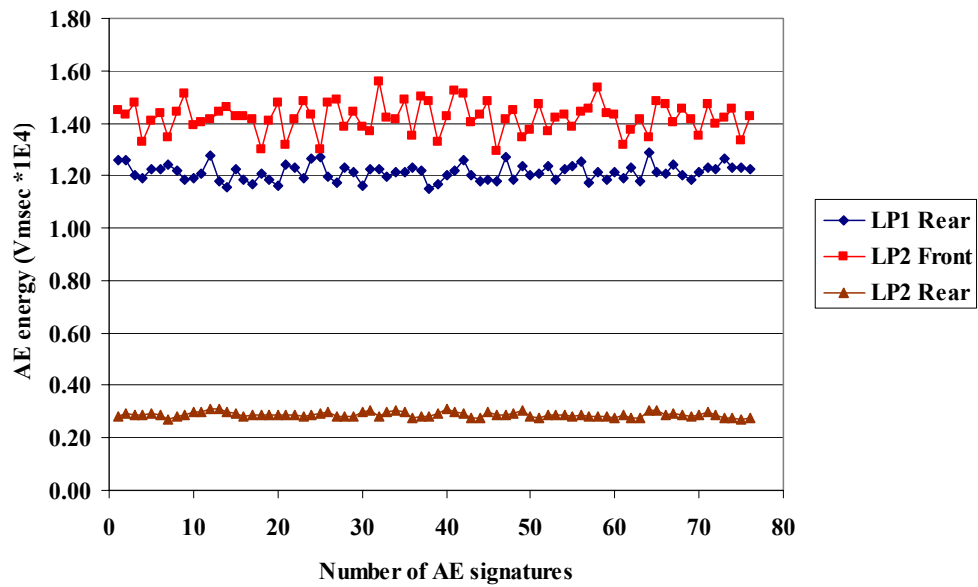


Figure 12 Comparison of AE energy levels

Comparison of AE amplitude levels from 'LP 2 Front and  
Rear' and 'LP 1 Rear'

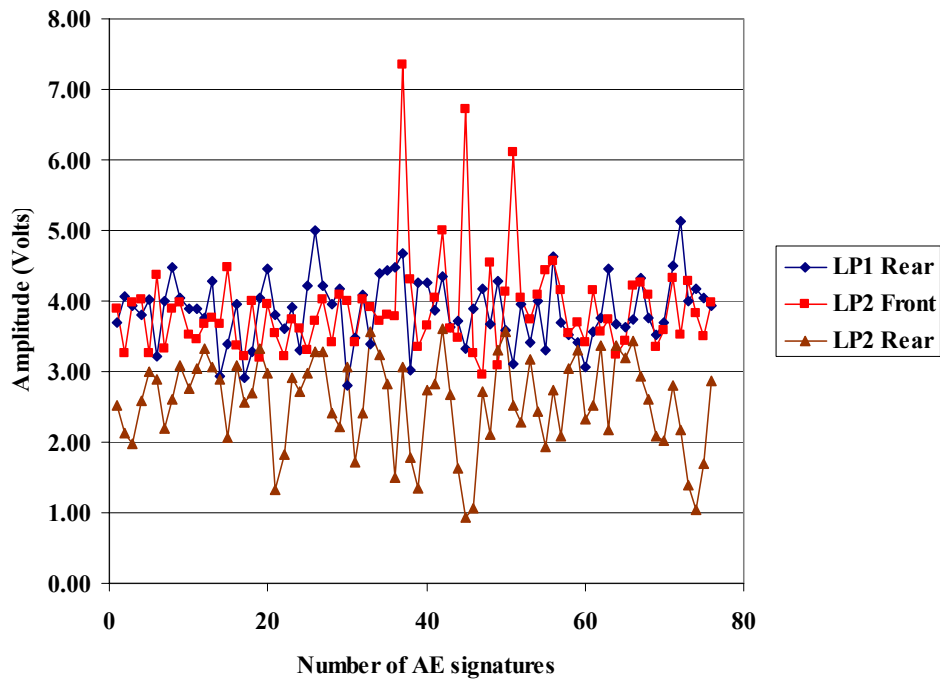


Figure 13 Comparison of maximum AE amplitude levels

## 7. Discussions

The strength (maximum amplitude and energy), duration and frequency content of signatures recorded on three seal/gland casings are indicative of an active AE source. It was also noted that the underlying background noise was in the order of  $\pm 0.5$  volt, as observed from 'LP2 Rear', see figure 3. Comparisons of AE energy and amplitude levels from 'LP2 Front and Rear' and 'LP1 Rear' provided an indication of the source of AE activity, see figures 12 and 13, and appendix A. Based on observations of AE energy and maximum amplitude values the likely source of AE activity was from either 'LP 2 Front' or 'LP1 Rear'. Whilst the AE amplitude levels at these positions were of similar magnitude, larger AE energy was evident at 'LP 2 Front'. Amplitude and energy levels for 'LP2 Front' and 'LP1 Rear' were greater than at 'LP2 Rear'. It was not possible to establish if there was only one AE source; 'LP2 Front' or 'LP1 Rear'. The coupling between these two positions ensured a direct transmission path for propagation of AE's across the turbine units. Therefore, if the source had been from either of these positions, 'LP2 Front' or 'LP1 Rear', it would be expected that the AE amplitude and energy levels detected at the other position would be much lower than observed values due to severe attenuation across the bearing/coupling. It was postulated that there were two sources of AE activity, hence two rubbing positions ('LP2 Front' and 'LP1 Rear').

As the low pressure cylinders were of identical size, and on the assumption that the transmission path to the receiving sensors are identical, it was observed that the strongest AE source was from 'LP2 Rear', and as such, it is highly probable that

rubbing of mating surfaces at this position was at a particular stage of wear that resulted in higher AE activity than at 'LP1 Rear'. The relationship between AE levels and wear has been investigated for sliding of lubricated and dry mating surfaces [18, 19, 20, 21, 22, 27]. Acoustic Emission activity was shown to be dependent on the asperity contact, surface roughness and third body interactions. It must be noted that although vastly researched, the interpretation of the wear/sliding mechanism that results in the generation of AE, and the strength of such emission, is still application specific and open to interpretation. The transient AE signatures detected at 'LP2 Rear' were attenuated signatures considered to be directly associated with 'LP2 Front'. Furthermore, as signatures were not detectable above the trigger level at 'LP1 Front', it confirmed that the strength of AE activity at 'LP1 Rear' was insufficient to be transmitted across the rotor and detectable above AE background noise levels.

It was thought prudent to filter the AE output signatures to ensure that the high frequency AE signatures, modulated at the rotational speed of the unit, was not attributed to excessively high vibrations overcoming in-built high pass filters of the acquisition system. This has been known to occur during AE diagnostic tests on operational bearing units (16). A digital elliptic filter with a band-pass frequency range of between 100kHz to 750kHz was applied to captured modulated AE signatures. The filter employed a 5dB loss limit in the pass-band and 60dB attenuation in the stop-band. A typical result before and after filtering can be seen in figure 14. It was concluded that the modulation was attributed to the high frequency AE signature.

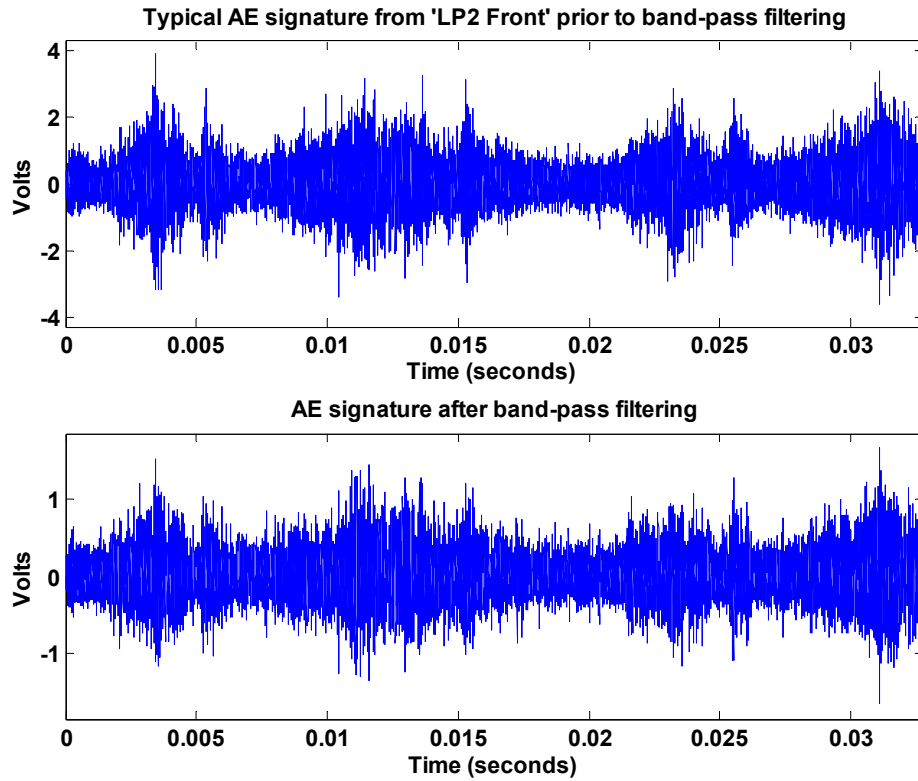


**Figure 14** Typical AE signature detected at ‘LP2 Front’ before and after band pass filtering.

Modulated high frequency AE waves, at the rotational speed of an operational turbine unit, had been observed by Sato [24]. However, in this investigation a twice-rotational speed modulation, particularly at ‘LP2 Front’, was observed. The author’s believe there are two probable reasons for this; firstly, there could exist two rubs at the seal/gland position. An AE signature modulated at the rotational speed of the unit is indicative of a continuous rub source. Such a rub type implies a sustained contact between the rotor and the stator, generating AE levels above operational background noise levels. The unbalance of the rotor will result in an increase in contact pressure at a periodicity equivalent to the rotational speed of the unit. The mechanism of a continuous rub will result in increasing AE energy and amplitude levels as a function of contact pressure and rotational position, creating the modulated high frequency AE

signature. This accounts for one rub type and it is postulated that the second rub was a partial rub from a seal removed from the exact location of the continuous rub but from the same seal/gland position. This intermittent generation of AE activity, superimposed on the modulated signature from the continuous rub is probably one reason for the observed twice-rotational speed modulation of the AE signature at 'LP2 Front'.

An alternative reason for the twice per revolution modulation of AE signatures was attributed to looseness of the spring rings used to retain the gland/seals in position. Any looseness of the spring rings will result in relative movement of the rings on the casing, generating AE activity. It is very probable that a rub, emitting a once-per-revolution modulation of high frequency AE signature, could be superimposed by a second once-per-revolution AE transient burst caused by the looseness of the spring rings, furthermore, it is likely that this latter AE source will be out of phase from the position of maximum contact pressure (maximum AE amplitude level). However, the scenario above is unlikely as AE signatures generated by relative movement between the casing and the springs must be transmitted back onto the rotor and across the unit such that AE signatures were detected at position 'LP2 Rear'. In light of the effects of attenuation, this prognosis is weak.

In any event, a measure of AE activity, modulated at the rotational speed of the unit, served to reinforce a suspected rub, particularly as a second visit showed no sign of such modulation. However, it was observed that the background noise during the second visit was much higher than the previous recordings and this is attributed to the change in operating characteristics. The implication of this is that operational

background noise influences the AE levels. This background noise is assumed to be ‘white noise’ and any rubbing between seals and the rotor will manifest as modulations of high frequency AE at a multiple of the shaft speed; also observed by Sato [24].

## **8. Conclusions**

- The modulation effect on the high frequency AE signatures detected at the gland/seal casings has been shown to aid verification of a suspected rub.
- In addition, the AE signatures highlighted the probability of two locations of rubbing which by using standard vibration analysis is a diagnosis that could not be possible.
- The potential for the application of high frequency AE analysis for diagnosing and verifying seal rubbing in power generating turbine units has been presented.

## **9. References**

1. A Muszynska, Rotor-Stationary element rub-related vibration phenomena in rotating machinery-Literature Survey, *The Shock and Vibration Digest*, 1989. **121**(3),3-11.
2. Ham, Trends and future scope in the monitoring of large scale steam turbine generators, *IEE proceedings*, 1986, **133**(3), Pt B.

3. Cotgrove, R.M.; Wood, M.I., Opportunities for advanced sensors for condition monitoring of Steam turbines, *IEE conference on Opportunities and Advances in International Power Generation*, March,1996, (Conf. Publ. No. **419**) , 119 -124.
4. Wevers, M. Fundamentals of Acoustic Emission, *22nd European Conference on Acoustic Emission Testing*, EWGAE, 29-31 May 1996, The Robert Gordon University, Aberdeen, 1- 11.
5. Mathews, J. R. *Acoustic emission*, 1983, Gordon and Breach Science Publishers Inc., NewYork. ISSN 0730-7152.
6. Pollock AA, *Acoustic Emission Inspection*, Physical Acoustics Corporation, Technical Report, TR-103-96-12/89,1989
7. Gorman M. R, Acoustic emission for the 1990s, *IEEE 1991 Ultrasound symposium proceedings*, 2, 1039.
8. Ono K, Recent Developments in Acoustic Emission, *Journal of Acoustic Emission*, 1996
9. Yoshioka T, Fujiwara T. Application of acoustic emission technique to detection of rolling bearing failure, *American Society of Mechanical Engineers*, Production Engineering Division publication PED, 1984, **14**, 55-76.
10. Rogers, L. M., The application of vibration analysis and acoustic emission source location to on-line condition monitoring of anti-friction bearings. *Tribology International*, 1979; 51-59.
11. Bagnoli, S., Capitani, R. and Citti, P. Comparison of accelerometer and acoustic emission signals as diagnostic tools in assessing bearing. *Proceedings of 2nd International Conference on Condition Monitoring*, London, UK, May 1988, 117-125.

12. Hawman, M. W., Galinaitis, W. S, Acoustic Emission monitoring of rolling element bearings, *Proceedings of the IEEE, Ultrasonics symposium*, 1988, 885-889
13. Tandon, N. and Nakra, B.C, Defect Detection of Rolling Element Bearings by Acoustic Emission Method, *Journal of Acoustic Emission*, 1990; **9**(1) 25-28.
14. Choundhury, A. and Tandon, N., Application of acoustic emission technique for the detection of defects in rolling element bearings, *Tribology International*, 2000, **33**, 39-45.
15. McFadden PD, Smith JD, Acoustic emission transducer for the vibration monitoring of bearings at low speeds. Report CUED/C-Mech/TR29, University of Cambridge, 1983.
16. Mba, D., Bannister, R.H., and Findlay, G.E. Condition monitoring of low-speed rotating machinery using stress waves: Part's I and II. *Proceedings of the Inst Mech Engr* 1999; **213**(E): 153-185
17. N. Jamaludin, D. Mba, R. H. Bannister Condition monitoring of slow-speed rolling element bearings using stress waves. *Journal of Process Mechanical Engineering*, Pro. Inst. Mech Eng., 2001, **215**(E), Issue E4, 245-271.
18. Dornfield, D. and Handy, C. Slip detection using acoustic emission signal analysis, *Proc IEEE Int. Conf. on Robotics and Automation*, 1987, 1868-1875.
19. Lingard, S. Sliding wear studies using acoustic emission-A short communication, *Wear*, 1993, **162**, 597
20. Bones R.J. and McBride, S. L., Adhesive and abrasive wear studies using acoustic emission techniques. *Wear*, 1991, **149**, 41-53
21. Boness, R.J., McBride, S.L., and Sobczyk, M. Wear studies using acoustic emission techniques. *Tribology International*, 1990; **23**(5): 291-295.

22. Hisakado T and Warashina T, Relationship between friction and wear properties and acoustic emission characteristics: iron pin on hardened bearing steel disk. *Wear*, 1998, **216**, 1-7.
23. Mba, D, Hall, L. The transmission of Acoustic Emission across large-scale turbine rotors. *NDT and E International*, 2002, **35**(8), 529-539.
24. Sato, I., Rotating machinery diagnosis with acoustic emission techniques, *Electrical engineering in Japan*, 1990, 110(2), 115-127.
25. Board, C. B. Stress wave analysis of turbine engine faults, *Aerospace Conference Proceedings, IEEE*, 2000, **6**, 79 -93.
26. Wang, Q and Chu, F. Experimental determination of the rubbing location by means of acoustic emission and wavelet transform. *Journal of Sound and Vibration*, 2001, **248**(1), 91-103
27. Miettinen, J and Siekkinen, V. Acoustic emission in monitoring sliding contact behaviour. *Wear*, 1995, **181**, 897-900

**Appendix A AE values of maximum amplitude and energy measured at ‘LP1 Rear’, and ‘LP2 Front and Rear’**

File no.	<u>MAX. AMPLITUDE</u>		
	LP1 Rear	LP2 Front	LP2 Rear
1	3.70	3.89	2.51
2	4.06	3.27	2.13
3	3.93	3.97	1.99
4	3.79	4.02	2.58
5	4.02	3.26	3.01
6	3.21	4.38	2.90
7	4.01	3.32	2.19
8	4.48	3.89	2.62
9	4.03	3.98	3.08
10	3.89	3.53	2.76
11	3.90	3.45	3.05
12	3.76	3.68	3.32
13	4.28	3.76	3.07
14	2.94	3.68	2.88
15	3.39	4.47	2.07
16	3.96	3.37	3.10
17	2.91	3.21	2.56
18	3.28	3.99	2.70
19	4.04	3.19	3.32
20	4.46	3.96	2.98
21	3.80	3.54	1.32
22	3.60	3.23	1.83
23	3.92	3.75	2.91
24	3.31	3.62	2.72
25	4.21	3.31	2.99
26	5.01	3.72	3.29
27	4.21	4.01	3.29
28	3.97	3.41	2.41
29	4.18	4.10	2.22
30	2.81	4.00	3.06
31	3.48	3.41	1.71
32	4.09	4.01	2.42
33	3.40	3.91	3.57
34	4.39	3.72	3.25
35	4.44	3.80	2.82
36	4.47	3.79	1.51
37	4.68	7.35	3.07
38	3.01	4.30	1.78
39	4.27	3.35	1.36
40	4.26	3.65	2.74
41	3.88	4.04	2.83
42	4.35	5.01	3.60

<u>ENERGY</u>		
LP1 Rear	LP2 Front	LP2 Rear
*1e4	*1e4	*1e3
1.26	1.45	2.82
1.26	1.43	2.93
1.20	1.48	2.87
1.19	1.33	2.86
1.23	1.41	2.94
1.23	1.44	2.88
1.24	1.35	2.70
1.22	1.45	2.84
1.19	1.51	2.88
1.19	1.39	2.98
1.21	1.41	3.00
1.28	1.41	3.09
1.18	1.44	3.11
1.16	1.46	2.96
1.23	1.43	2.91
1.18	1.42	2.79
1.17	1.41	2.88
1.21	1.30	2.88
1.18	1.41	2.88
1.16	1.48	2.89
1.24	1.32	2.86
1.23	1.42	2.87
1.19	1.49	2.81
1.27	1.43	2.90
1.27	1.30	2.94
1.20	1.48	2.99
1.17	1.49	2.80
1.23	1.38	2.80
1.22	1.44	2.81
1.16	1.39	2.99
1.23	1.37	3.03
1.23	1.56	2.79
1.20	1.42	2.96
1.21	1.41	3.03
1.21	1.49	2.97
1.23	1.35	2.78
1.22	1.50	2.83
1.15	1.48	2.82
1.17	1.33	2.92
1.20	1.43	3.12
1.22	1.52	2.99
1.26	1.51	2.91

File no.	<u>AMPLITUDE</u>		
	LP1 Rear	LP2 Front	LP2 Rear
43	3.63	3.61	2.68
44	3.71	3.47	1.62
45	3.33	6.71	0.93
46	3.89	3.27	1.06
47	4.18	2.95	2.71
48	3.67	4.55	2.10
49	4.27	3.08	3.31
50	3.59	4.14	3.56
51	3.11	6.12	2.51
52	3.96	4.05	2.28
53	3.42	3.75	3.17
54	3.99	4.09	2.43
55	3.31	4.42	1.94
56	4.63	4.57	2.74
57	3.69	4.15	2.09
58	3.52	3.55	3.04
59	3.41	3.70	3.30
60	3.06	3.41	2.33
61	3.56	4.16	2.52
62	3.76	3.57	3.37
63	4.45	3.74	2.18
64	3.67	3.25	3.36
65	3.63	3.43	3.19
66	3.74	4.21	3.44
67	4.34	4.25	2.93
68	3.75	4.08	2.60
69	3.52	3.35	2.09
70	3.69	3.59	2.01
71	4.51	4.32	2.81
72	5.13	3.52	2.17
73	4.00	4.28	1.39
74	4.18	3.82	1.04
75	4.04	3.50	1.69
76	3.93	3.97	2.87

<u>ENERGY</u>		
LP1 Rear	LP2 Front	LP2 Rear
*1e4	*1e4	*1e3
1.20	1.40	2.76
1.18	1.43	2.76
1.18	1.48	2.97
1.18	1.30	2.89
1.27	1.42	2.89
1.18	1.45	2.94
1.23	1.35	3.06
1.20	1.37	2.80
1.21	1.47	2.77
1.23	1.37	2.87
1.19	1.42	2.90
1.22	1.43	2.89
1.24	1.39	2.82
1.25	1.44	2.88
1.17	1.45	2.79
1.21	1.53	2.83
1.18	1.44	2.84
1.21	1.43	2.78
1.19	1.32	2.88
1.23	1.37	2.77
1.18	1.42	2.79
1.29	1.35	3.06
1.21	1.48	3.05
1.21	1.47	2.86
1.24	1.40	2.91
1.20	1.46	2.86
1.19	1.41	2.81
1.21	1.35	2.86
1.23	1.47	3.00
1.22	1.40	2.87
1.27	1.42	2.77
1.23	1.46	2.74
1.23	1.34	2.69
1.22	1.42	2.77